Early life stress impairs postnatal oligodendrogenesis and adult behavior through activity-dependent mechanisms.

Teissier A. [1,2], Le Magueresse C. [1], Andrade da Costa B. [3], Olusakin J. [1], De Stasi A.M. [4], Bacci A. [4], Kawasawa Y.I. [5], Vaidya V.V. [6], Gaspar P. [1]

[1] INSERM, Institut du Fer à Moulin, U839 Sorbonne Université, Paris, France

[2] Institut Jacques Monod, CNRS UMR 7592, Université Paris Diderot, France

[3] Pharmacology Department, Federal University of Pernambuco, Recife, Brazil

[4] Institut du Cerveau et de la Moelle épinière, CNRS UMR 7225 – Inserm U1127, Sorbonne Université, Paris, France

[5] Departments of Pharmacology and Biochemistry and Molecular Biology, Institute for Personalized Medicine, Penn State University College of Medicine, Hershey, Pennsylvania, USA

[6] Department of Biological Sciences, Tata Institute of Fundamental Research, Mumbai 400005, India

ABSTRACT (max 250 words)

Exposure to stress during early life (infancy/childhood) has long-term effects on the structure and function of the prefrontal cortex (PFC) and increases the risk for depression and anxiety disorders. However, little is known about the molecular and cellular mechanisms of these effects. Here we focused on changes in a mouse model of early stress induced by chronic maternal separation (MS). Unbiased mRNA expression profiles in the medial PFC (mPFC) of MS pups (P15) identified an increased expression of myelin-related genes and a decreased expression of immediate early genes. We further analyzed oligodendrocyte lineage markers and performed birthdating experiments to show a precocious oligodendrocyte differentiation in the mPFC of MS pups that led to a depletion of the oligodendrocyte progenitor pool in adults. Pharmacogenetic inhibition of neuronal activity in the developing mPFC of control animals induced a similar premature differentiation of the oligodendrocyte lineage, while the transient increase of mPFC activity in MS pups prevented this change. Moreover, the developmental diminution of mPFC activity mimicked the emotional and cognitive phenotypes observed in MS, while activating the mPFC during MS prevented the emergence of depression and cognitive disorders in adulthood. Altogether, our results identify an activity-dependent maturation process in the developing mPFC that is influenced by early life stress and has critical functions on postnatal oligodendrogenesis as well as adult emotional and cognitive behaviors.

INTRODUCTION

The environment a child encounters during early life plays a critical role in normal brain development. It has been repeatedly documented that early life stress (ELS), which includes various forms of child abuse and neglect, increases the risk to develop psychiatric disorders [1–4]. Accordingly, brain imaging studies in patients exposed to childhood adversity show altered brain activity and myelin content, notably affecting the medial prefrontal cortex (mPFC) which constitutes a critical hub for emotional control and cognition [5–8]. However, the developmental mechanisms underlying these long-term effects of early stress remain unclear.

To identify the pathophysiological mechanisms leading to ELS phenotypes, in particular as regards to mood and anxiety disorders, several preclinical models have been developed [9,10]. The most commonly used rodent model of ELS involves daily maternal separation (MS) during the early postnatal period, a time when pups normally spend most of their time huddled in the mother's nest [9,11]. Rodents exposed to MS during the first postnatal weeks display, as adults, a permanent impairment of emotional and cognitive behaviors, together with an altered physiology, cytoarchitecture, and myelination of the mPFC [12–15]. Strikingly, these behavioral and structural defects closely reproduce the phenotypes of humans exposed to childhood trauma [10,16]. Several of these alterations are already apparent at juvenile or adolescent stages [14,17–20] but the causal mechanisms remain poorly understood.

A critical role of neuronal activity in cortical maturation has been demonstrated in the primary sensory cortical maps (visual, somato-sensory, auditory) [21,22] in which the activity of the incoming axons can be easily manipulated. In these classical model systems, neuronal activity has been shown to play critical roles, not only in the maturation of excitatory and inhibitory synaptic connections, but also in the onset of myelination that marks the stabilization of brain circuits. Activity thus appears as the mechanistic link between changes in the environment and alterations in the brain's developmental trajectory. We hypothesize that similar influence of neuronal activity likely exists in associative cortices such as the mPFC. Supporting this hypothesis, recent electrophysiological recordings and molecular analysis showed that maternal care modulates neuronal activity in mPFC [14,18,23,24]. However, the role of neuronal activity during critical periods of PFC development has not been tested yet.

In the present study, we focused on cellular and molecular changes occurring in the mPFC at the outset of ELS. We started with an unbiased transcriptome screen in the mPFC, comparing MS with standard facility raised (SFR) pups. Unexpectedly, we identified major changes in gene pathways associated with myelination and neuronal activity. Turning to cellular analyses, we documented a precocious differentiation of oligodendrocyte progenitor cells (OPC) in MS P15 pups, which coincided with an increase in myelin transcripts. Conversely, the OPC pool was depleted in adults. To determine the role of activity in these phenotypes, we manipulated locally mPFC neuronal activity in pups using designed receptors exclusively activated by designed drugs (DREADDs) [25]. We found that local and transient decrease in neuronal activity is sufficient to induce premature OPC differentiation, while the transient increase in neuronal activity prevents it. Additionally, we demonstrate that the emotional and cognitive disorders induced by ELS in adulthood are controlled by developmental changes in mPFC neuronal activity. Taken together, our results demonstrate a fundamental role of mPFC postnatal activity in the etiology of ELS behavioral phenotypes and identify oligodendrogenesis as a potential underlying mechanism in this process.

RESULTS

Early life stress (ELS) alters the expression of immediate early genes and genes involved in myelin formation in the developing medial prefrontal cortex (mPFC).

As a preclinical model of ELS, we used the common model of chronic maternal separation (MS), where pups are daily separated for 3h from their dam starting at postnatal day 2 (P2) and until P14 (Figure 1A) [11,15]. To identify early molecular candidates potentially involved in the

permanent alterations induced by ELS, we focused on the chronic effect of MS by analyzing P15 mPFC, sampled 24h after the last maternal separation, and we performed an unbiased genetic screen using high throughput RNA sequencing. To minimize inter-individual variations and dissection biases, mPFC of 3 males from different litters were pooled and 4 independent samples per condition were tested. After normalization by the RUVSeq R package v3.1 [26] and using edgeR, we found a total of 86 genes differentially expressed between MS and SFR animals (adjusted p value <0.05 and change in transcript level >30%, Supplementary Table 1). Among the 56 up-regulated genes, Gene Ontology (GO) analyses revealed a major enrichment in biological processes related to myelin ensheathment and oligodendrocytes differentiation (red dots in Figure 1B and Supplementary Figure 1). Similar analyses of the 30 down-regulated genes displayed enrichment in cellular response to calcium (Supplementary Figure 1) likely due to the strong representation of several immediate early genes (IEG) (blue dots in Figure 1B). To validate these changes we performed quantitative PCRs on mPFC mRNAs obtained from a new cohort of MS and SFR animals analyzed at P15. This second cohort confirmed the decrease in IEG transcripts (*Fos*, *Fosb* and *Arc*, Figure 1C) and the increase in myelin-related transcripts (*Mag*, *Mog* and *Plp1*, Figure 1D). Altogether, this unbiased approach identified for the first time an early concomitant alteration of transcripts related to IEG and myelin ensheathment in the mPFC of postnatal animals exposed to chronic maternal separation.

Premature OPC differentiation in ELS pups.

To determine possible causes of the increase in myelin related transcripts, we investigated oligodendrogenesis in MS animals. The postnatal period corresponds to an intense proliferation of oligodendrocyte progenitors cells (OPC) and, P15 marks the initiation of differentiation into myelinating oligodendrocytesin the mPFC [20,27]. We performed triple immunostaining of Olig2, PDGFRα and CC1 to distinguish OPC ($Olig2^+PDGFR\alpha^+$, Figure 2A) from differentiated oligodendrocytes (OL, $Olig2^+CC1^+$) [28]. At P15, we observed a significant increase in the density of OL in the mPFC of MS animals compared to SFR animals ($F(1,7)=21.84$ $p=0.0023$), while the density of OPC was unaltered ($F(1,7)=0.032$ $p=0.863$, Figure 2B). At adult stages, we observed a significant decrease in OPC density ($F(1,8)=6.28$ $p=0.036$), while no difference in OL was detected ($F(1,8)=0.022$ $p=0.8865$, Figure 2C). To test whether early differentiation contributes to these observations, sequential staining of the dividing progenitors was performed using two thymidine analogs at P10 (iodo-deoxyuridine, IdU) and P15 (bromo-deoxyuridine, BrdU, Figure 2D). This interval was chosen because OPC differentiate into OL in approximately 5 days [27]. In the mPFC of P15 MS animals, the fraction of OPC that kept dividing between P10 and P15 (triple labeled with $Olig2^+IdU^+BrdU^+$, blue bars in Figure 2E, $F(1,5)=12.62$ $p=0.0163$) was significantly reduced, while the differentiating fraction ($Olig2^+IdU^+BrdU^-$, purple bars, $F(1,5)=7.234$ $p=0.0433$) was increased. Thus, our results demonstrate that MS induces a precocious differentiation of the OPC pool during development, as a potential cause for depletion of the OPC pool in adults. To assess how oligodendrogenesis defects could be related with the alterations in IEG we previously observed, we performed immunostaining on P9 MS mPFC (Supplementary Figure 2). We noticed that the decrease in IEG expression preceded the defects in oligodendrogenesis thus suggesting a chronic down-regulation of neuronal activity in the MS pups. Considering the important role of neuronal activity in adult myelination [29], we further tested how manipulation of neuronal activity over the early postnatal period could modify oligodendrogenesis.

Pharmacologic manipulation of mPFC postnatal activity bi-directionally controls developmental oligodendrogenesis.

We used viral delivery of AAVs expressing DREADDs to transiently and bi-directionally manipulate neuronal activity in the mPFC [25,30]. AAV8-hSyn-hM4Di-mCherry or AAV8-hSyn-hM3Dq-mCherry viral constructs were bilaterally injected into the mPFC of all P1 pups (Figure 3A) and they further received daily injections of saline (SAL) or the inert ligand Clozapine-N-Oxyde (CNO) from P2 to P14. Pups injected with the inhibitory construct were raised in the SFR condition (referred to as SFR+hM4Di, Figure 3A). Conversely, pups injected with the activatory construct were submitted to the MS protocol (referred to as MS+hM3Dq). We first verified the timing and efficiency of expression. mCherry expression in cortical neurons was visible 36h after injection (at P2.5, data not shown) and at P15, 38%±5.2 of mPFC NeuN$^+$ cells were mCherry$^+$ upon hM4Di injections and 51.8%±4.4 upon hM3Dq injections. In addition, 95,98%±0.06 of the mCherry$^+$ cells were NeuN$^+$, 72,59%±3.75 were Tbr1$^+$ or Ctip2$^+$ and only 6.17%±1.24 were GABA$^+$ (Figure 3B-C). No co-expression of mCherry with Olig2 or PDGFRα or the oligodendrocyte-specific antibody CC1 could be detected (data not shown) supporting that viral infections essentially targeted neurons, with a bias for deep-layer glutamatergic neurons (Tbr1$^+$ or Ctip2$^{+)}$.

To evaluate the efficiency of the DREADD constructs, we used *ex vivo* patch clamp electrophysiological recordings. We observed a robust increase in neuronal excitability upon exposure to CNO (30µM) or to its potential metabolite clozapine (1µM), in hM3Dq-mCherry$^+$ layer 5 pyramidal neurons from P10 mPFC (Supplementary Figure 3). In hM4Di-mCherry$^+$ neurons, exposure to CNO or clozapine did not modify neuronal excitability (Supplementary Figure 3), which may be due to the preferential pre-synaptic targeting of hM4Di in cortical neurons [30,31] and to the low expression of G protein-coupled inwardly-rectifying potassium (GIRK) channels in the cortex at this age [32]. Of note, we observed a significant difference in excitability between hM4Di-mCherry$^+$ and hM3Dq-mCherry$^+$ cells in the absence of any ligand, suggesting that hM3Dq DREADDs are partially activated in basal conditions ($p<0.0001$ $F(6,144)=85.479$, see controls in Supplementary Figure 3B and 3D). Nevertheless, the inhibitory action of hM4Di was demonstrated by a significant decrease in mPFC Egr1 expression among hM4Di-mCherry$^+$ neurons, in P8 and P15 animals sacrificed 2 hours after CNO injection (Supplementary Figure 3). Additionally, a sustained decrease in cFos labeling was observed in P15 mPFC of SFR+hM4Di mice sacrificed 24h after chronic CNO exposure (P2-P14), while a sustain increase was observed in P15 MS+hM3Dq mice (Supplementary Figure 3). Altogether, these results support the efficacy of our approach for mimicking or preventing the chronic decrease in IEG expression in the mPFC induced by MS during the postnatal period.

To test whether changes in early neuronal activity play a causal role in the MS-induced oligodendrogenesis defects, P15 and adults brains were analyzed after SFR+hM4Di or MS+hM3Dq treatments, as described above. We found an increased density of OL at P15 ($F(1,7)=15.991$ $p=0.005$, Figure 3D), and a decrease density of OPC in adults ($F(1,9)=7.809$ $p=0.0209$, Figure 3E) in SFR+hM4Di animals after P2-P14 CNO exposure. Conversely, we found an increase in the density of OPC at P15 in MS+hM3Dq animals with P2-P14 CNO exposure ($F(1,7)=6.52$ $p=0.0379$, Figure 3F), that was followed by a late increase in OL density ($F(1,8)=25.795$ $p=0.001$, Figure 3G). Therefore, transient inhibition of mPFC neurons reproduced

the oligodendrogenesis defects of mice exposed to MS, suggesting early exit of the cell cycle. On the other hand, transient activation of the mPFC was sufficient to prevent the MS-induced defects in oligodendrogenesis. These results indicated a causal role of altered mPFC neuronal activity on the precocious oligodendrogenesis observed in MS animals.

Postnatal local decrease in mPFC activity recapitulates MS behavioral phenotype in adults.

Adult animals exposed to MS have been shown to display behavioral phenotypes, such as increased depression and cognitive deficits, suggestive of alterations in mPFC development. We tested the causal role of developmental pharmacologic manipulations in the PFC on these phenotypes. Because variability in MS effects in different mouse strains has been reported [11], we began with a characterization of the behavioral phenotype of adult BALBcJ mice exposed to chronic MS (Figure 4A). In our protocol, MS males showed decreased exploration (Mann-Whitney p=0.0002) and time spent in the center in the open field (OF, F(1,25)=4.317 p=0.0482, Figure 4B and C) as well as decreased time spent in the open arm of the elevated plus maze (EPM, F(1,22)=5.438 p=0.0293, Figure 4D). They further showed an increased burying behavior in the marble test (F(1,32)=5.402 p=0.0266, Figure 4E), when compared with SFR animals. In addition, MS males displayed an increased time floating in the forced swim test (FST, F(1,26)=6.048 p=0.0209, Figure 4F) and an impaired working memory in the sequential novel object recognition test (SNOR, F(1,23)=4.75 p=0.0396,) which measures the preference in exploring an object seen less recently than another [18,33]. These results confirmed an increase in anxiety and depression-related behaviors in MS animals and impaired in a working memory task highly linked to mPFC functioning [33].

Strikingly, adults SFR+hM4Di animals exposed to P2-P14 CNO exhibited behavioral alterations very similar to those of MS animals, when compared with SAL treated animals. These included reduced exploration of the OF (distance F(1,24)=6.433 p=0.0181, Figure 4B' and center time F(1,24)=4.46 p=0.0452, Figure 4C'), reduced exploration of the EPM (F(1,22)=9.94 p=0.0067, Figure 4D'), increased burying in the marble test (F(1,26)=5.233 p=0.305, Figure 4E'), and increased floating in the FST (F(1,26)=5.675 p=0.0248, Figure 4F') and decreased preference in the SNOR test (F(1,19)=4.443 p=0.0485, Figure 4G'). They also show delayed postnatal growth with a sustained decreased in adult weight, as observed in MS animals (Supplementary Figure 4). As an additional control, to exclude any unwarranted effects of the effects of chronic exposure to CNO, a P2-P14 CNO/SAL cohort of animals was tested for adult behavior and showed no behavioral change (Supplementary Figure 5). Altogether, our data show that decreased mPFC activity during development is sufficient to recapitulate salient features of the adult's MS phenotype.

The postnatal local increase in mPFC activity prevents the emergence of depression-related MS phenotype.

To test for the requirement of altered mPFC activity in MS behavioral phenotype, we assessed the behavior of animals exposed to the MS protocol with or without chemogenetic activation (hM3Dq) of the mPFC (Figure 5A). When compared to SAL-treated MS animals, CNO treated MS mice did not show a difference in the behavioral parameters related to anxiety, including: the

distance or the time in the center of the OF (Figure 5B, F(1,32)=0.604 p=0.4427 and C, F(1,32)=1.397 p=0.246), the time in the open arm of the EPM (Figure 5D, F(1,33)=2.002 p=0.1664) or the number of burying in the marble test (Figure 5E, F(1, 32)=1.656 p=0.2074). However, CNO exposed MS+hM3Dq animals floated less in the FST (Figure 5F, F(1,29)=6.508 p=0.0163) and display an improved performance in the working memory-test (Figure 5G, Mann-Whitney p=0.0463). To strengthen our analysis of the depression-related phenotype we used the sucrose splash test, which measures self-care and hedonic behaviors [34]. We observed an increased grooming behavior in CNO exposed MS+hM3Dq animals as compared to SAL (Figure 5H, F(1, 25)=6.532 p=0.171). Conversely, animals solely exposed to MS display a decrease in grooming when compared with SFR animals (Figure 5I, F(1,25)=5.618 p=0.0258). Hence, transient mPFC activation prevented the emergence of the depression and cognitive aspects of MS phenotypes, but not of the anxiety-related aspect.

DISCUSSION:

Using an unbiased approach, we identified predominant alterations in plasticity and myelin–related genes within the maturing mPFC of an early life stress model. Our analysis of the oligodendrocyte lineage showed a precocious differentiation upon MS and a subsequent depletion of the OPC pool in adult brains. We took advantage of pharmacogenetic tools to further establish that a transient and local alteration of mPFC neuronal activity during postnatal development was sufficient to recapitulate or prevent the defects in oligodendrogenesis and in mood behaviors induced by MS. Our results thus demonstrate a direct role of postnatal mPFC activity in the etiology of emotional and cognitive neurodevelopmental disorders and raise the possibility that postnatal oligodendrogenesis is involved in this process.

The pre-weaning period is critical for mPFC myelination

We found that MS (P2-P14) induces a significant increase in the expression of myelin-related genes at P15, correlating with a precious differentiation of the oligodendrocyte lineage and permanent alterations of the adult OPC pool. These results identify P2-P14 as a critical period for oligodendrogenesis in the mPFC, which coincides with the critical period for emotional behaviors, including mood and anxiety disorders [35,36]. Previously, another critical period for oligodendrogenesis has been identified at juvenile stages (P21-P35) when transient social isolation induces permanent deficit in adult social interactions associated with decreased myelin content and OPC proliferation [37]. Of note, adult exposure to various chronic stress has only transient consequences on behavior and mPFC myelination [37–39]. Therefore, our results, by showing the importance of the P2-P14 period, suggest that successive and/or expanded critical period(s) occur in the mPFC to establish anxiety, mood and social circuits. These two postnatal periods correspond to different stages of oligodendrogenesis that could be differentially affected by stressors although both result in decreased myelin content in mPFC at adult stages [12,20].

The developmental mechanisms involved in adult hypomyelination after MS are still disputed [7,12]. Our data favor a precocious differentiation of the oligodendrocyte lineage resulting in a depletion of the OPC pool in adults. This interpretation is supported by a recent clinical paper indicating that childhood adversity in human biases oligodendrocyte lineage toward a more differentiated phenotype in the vmPFC, with more pronounced effects in samples from young

individuals that died closer to ELS experience [7]. In addition, several other studies of sensory deprivation during critical periods or exposure to early life stress similarly reported, in other brain structures than mPFC, a transient and immediate increase in myelin content followed by a permanent decrease in adulthood [40–44]. However, another study by Yang et al. [20] reported a deficit in OPC differentiation when studying effects of MS in the mPFC of Sprague Dawley rats. The discrepancy with the present results could be due to a number of technical differences such as species, and timing of analysis and proliferation labeling. Identifying the precise mechanisms by which ELS affects oligodendrogenesis should ultimately clarify this debate, while overall these data support critical effects of MS on oligodendrocyte maturation processes.

Neuronal activity controls early stages of oligodendrogenesis

Recent advances have established an important role for experience and neuronal activity in controlling adult oligodendrogenesis and myelination [29]. Additionally, our unbiased approach identified an important decrease of several IEG in the P15 mPFC after MS, as a proxy for a deficit in neuronal plasticity [45]. Converging reductions of *Fos* and *FosB* further suggest that there is a chronic dampening of neuronal network activity in the mPFC. These results are in agreement with previous reports in the rat MS model showing a local decrease in specific IEG expressions and a reduced neuronal synchrony in the mPFC, as revealed by *in vivo* recordings [14,18].

We further demonstrate that stimulation of neuronal activity in the developing mPFC favors OPC proliferation at the expense of differentiation and prevents the emergence of oligodendrogenesis defects induced by MS. Conversely, chronically decreasing activity induces a bias toward OPC differentiation, thus mimicking the MS phenotype. To the best of our knowledge, this is the first demonstration of a causal role of neuronal activity on mPFC oligodendrogenesis and on postnatal oligodendrogenesis. Nevertheless, in adults, increased neuronal activity stimulates proliferation and differentiation of OPC and increases myelination in the long run [29,46,47]. This is therefore opposite to the effect that we observe during early postnatal life, since we show that increased neuronal activity stimulates proliferation at the expense of differentiation. Our results suggest that early stressors induce a pathological precocious differentiation which thereafter alters myelin content, or the capacity of myelin plasticity in adult life. Therefore, different activity-dependent regulations of oligodendrogenesis could be at play during development. This is supported by changes in the molecular properties of OPCs during this postnatal period [48,49], including the establishment of transient synaptic connectivity between OPCs and interneurons [29,50].

Early neuronal activity as a common regulator for psychiatric disorders?

Another important finding of the present study is the direct role of activity during critical periods of early life, for the etiology of emotional and cognitive disorders. The fundamental role of the excitatory/inhibitory balance in the establishment of critical periods has been identified in all primary sensory cortices [21,51,52]. Our study provides the first clear demonstration that locally modifying mPFC neuronal activity during a critical period durably affects adult emotional behavior. The mPFC neuronal network is still being assembled during the postnatal period, in particular with the maturation of outgoing and cortico-cortical glutamatergic and GABAergic circuits. Since our pharmacogenetic approach targeted both types of neurons, it remains to be determined how this affects circuit refinement. However, on a translational perspective, our

results demonstrate that early mPFC activity tightly controls two major MS-related endophenotypes, namely oligodendrogenesis and depression-related behavior, thus establishing a common cause for these typical traits of emotional disorders [53–55]. A direct role of oligodendrogenesis activity in the etiology of emotional disorders has previously been suggested by recent studies in adults reporting emotional deficits after genetic alterations of oligodendrogenesis [37,56–60]. Another line of evidence showed that the social avoidance induced by chronic stress correlate with myelin alterations in the mPFC and that restoring myelination is sufficient to rescue it, hence reinforcing the correlations between myeline defects and behavioral defects [39,61]. Present results establish a critical role of mPFC postnatal neuronal activity in the etiology of ELS behavioral alterations, and further support an implication of early oligodendrogenesis in adult behavior.

MATERIAL AND METHODS

Animals

All experiments performed in mice were in compliance with the standard ethical guidelines (European Community Guidelines and French Agriculture and Forestry Ministry Guidelines for Handling Animals-decree 87849). All dams were first-time pregnant BALB/cJ Rj mothers shipped from Janvier Labs ~ 7 days before delivery. At arrival, pregnant females were group-housed by 2 and litters sizes were homogenized from 8 to 14 animals with both genders represented. After weaning at P21, all the mice were group-housed (4-5 per cage), and kept under standard laboratory conditions (22 ± 1°C, 60% relative humidity, 12-12 hrs light–dark cycle, food and water *ad libitum*) in ventilated racks. Males and females were similarly exposed to maternal separation protocol (MS) and/or viral injections, but only males were used for results while females were sacrificed at weaning except for: (i) the first cohort of MS animals where both genders were behaviorally tested, (ii) females exposed to P1 viral injection were sacrificed at P8 or P14 to test for CNO efficacy using Egr1 staining, and (iii) a cohort of SFR females exposed to chronic postnatal CNO.

Maternal Separation Protocol:

Maternal separations (MS) of pups from their dams were conducted daily between 1:00 and 4:00 P.M., starting at postnatal day 2 (P2) and terminating at P14. Briefly, dams were first removed from the home cage and placed into a clean cage, then pups, were collected and placed together into another clean cage. The two cages were distanced to avoid vocalizations. After the 180 min, pups and then dams were returned to their home cage. Control animals were standard facility-reared (SFR) and did not receive extra handling. Animals were sexed at P1 to allow homogeneous distribution of males and first cage change occurred at P2, then every week.

RNA-sequencing

For the transcriptomic profiling, bilateral mPFCs from SFR (n=12) and MS (n=12) animals were dissected manually at P15 (Figure 1), fast frost on dry ice and collected in 100 µL of RNALater® (Ambion, Life Technology). 3 unilateral mPFCs from different litters were pooled to generate 4 samples by treatments that were shipped to Penn State Hershey Genome Sciences Facility. Total RNA was extracted using mirVana kit (Thermo Fisher Scientific) and a bead mill homogenizer (Bullet Blender, Next Advance) together with an equivalent mass of stainless steel beads (Next Advance) were used to homogenize the tissue. The cDNA libraries were prepared using

SureSelect Strand Specific RNA Library Preparation Kit (Agilent Technologies) and RNA and cDNA qualities were assessed using BioAnalyzer Kits (Agilent Technologies, RNA 6000 Nano and High Sensitivity DNA). The 12 libraries were loaded onto TruSeq SR v3 flow cells on an Illumina HiSeq 2500 and run for 50 cycles using a single-read recipe (TruSeq SBS Kit v3). The Illumina CASAVA pipeline Version 1.8 was used to extract de-multiplexed sequencing reads and FastQC (version 0.11.2) was used to validate the quality of the raw sequence data. Additional quality filtering was performed using FASTX-Toolkit with a quality score cutoff of 20. Next, alignment of the filtered reads to the mouse reference genome (mm10mm10) was done using Tophat (version 2.0.9) allowing 2 mismatches. Raw read counts were calculated using HTSeq-count [62]. The "remove unwanted variation" (RUVg) strategy ("RUVseq" R package, v3.1) as described by Risso et al. [26] was used along with edgeR [63] to identify differentially expressed genes (DEG) between MS and SFR animals. First we normalized the raw read counts by selecting a set of "in-silico empirical" negative controls, i.e., 5000 least significantly DEG genes based on a first-pass DEG analysis performed prior to normalization. Normalized read counts were applied using the negative binomial GLM approach implemented in edgeR using the Likelihood Ratio Test method. Significantly DEG were defined to be those with q-value < 0.05 calculated by the Storey et al. method [64].

RT-qPCR

mPFC were dissected and homogenized in 1ml of TriReagent (Sigma) using a Polytron®PT13000D (Kinematica) and RNA were extracted according to standard protocols. Genomic DNA was removed by digestion with Amplification Grade DNase I (Sigma-Aldrich). First-strand cDNA was synthesized by reverse transcription of 5µg of total RNA with Superscript-II reverse transcriptase (Invitrogen) according to standard protocols. Reverse transcriptase was omitted in some samples as negative control. Relative expression levels of *Gapdh, Arc, Fos, Fosb, Mag, Mog and Plp1* mRNAs were determined by real time quantitative PCR (RT-qPCR) using Absolute SYBR Green Mix (ABgene) and sets of specific primers (Supplementary Table 2) on a 96 wells plate (Thermo Scientific AB-0600). Gene expression was normalized to mouse *Gapdh* mRNA expression. Data were analyzed with the 2–**Δ**Ct method on MxPro qPCR software (Agilent Technologies), and values are expressed as the mean of duplicates.

AAV injections in the PFC

AAV8-hSyn-hM3D(Gq)-mCherry or AAV8-hSyn-hM4D(Gi)-mCherry (Addgene #50474 and #44362) were used as specified. The titers were within the range: 10^{12}-10^{13} particles/mL. Injections were done on P1 mice pups anesthetized on ice (1minute or until the absence of pinch reaction) and kept on a frozen pad during all the procedure (max 8 min). The cages were put on a heat pad 30min before the onset of the experiment and litters were separated from the dams and put on another heated cage with some bedding right before the onset. Pups were put in prone position to maintain the skull flat and the skin covering the skull was gently opened with a single incision using a razor blade. The mPFC was targeted using as a reference the inferior cerebral vein (~2-3 mm posteriorly) and the superior sagittal sinus (~2mm laterally). Bilateral injections (200 nL each) were performed at 1.1 mm deep from the skull surface using a pulled glass capillary (30-50 µm tip diameter PCR micropipette, Drummond Scientific Company) mounted on a hydraulic micromanipulator MO-10 (Narishige, Japan). After injection, the opened skin on the

skull was sealed using tissue adhesive glue (Vetbond #1469, 3M, France) and pups were gently warmed up. All pups from the same litters were injected to avoid competition for feeding and they were returned altogether to homecage at the end of the procedure. Careful supervision was provided on the hours following the procedure to favor mother acceptance and re-glue the scare if necessary. Afterward, cages were returned to the normal facility and daily supervision was provided.

Chronic CNO injections:

Saline solution (SAL, 0.9% NaCl) or 5 mg/kg CNO + 0.9% NaCl solution were injected daily from P2 to P14, either subcutaneously (P2-P4) or ip (P5 onward). For SFR+hM4Di and PNSAL/PNCNO cohorts, injections occurred at 1 pm. For the MS+hM4Dq cohort, injections occurred at 4 pm at the end of the maternal separation period.

Tissue processing

For cortical ontogenetic analysis, mice were sacrificed at postnatal (P8-P15) and adult stages. All mice were anesthetized (Pentobarbital 0.5 mg/g) and fixed by intracardiac perfusion of 4% paraformaldehyde in 0.1 M phosphate-buffered (PB pH=7.2) using a peristaltic pump (Thermoscientific Masterflex). Brains were quickly removed, post-fixed overnight in the same fixative solution and cryoprotected 2 days in 30% sucrose containing 0.01% sodium azide. 35 µm-thick coronal sections were prepared using a cryostat (Leica) or a cryotome (Microm Microtech). Serial sections from the whole brain were collected as series of 6. Tissue sections were used immediately for immunohistochemistry, if not, they were stored at -20°C in cryoprotective solution (30% ethylene glycol and 30% sucrose in 0.1 M phosphate buffer, pH=7.4).

Immunohistochemistry

Immunolabeling techniques were used on free-floating sections, and all the washes and antibody incubations were performed in blocking solution containing 1% horse serum and 0.2% triton in PBS (PBST). Primary antibodies were applied for 24 h (or 48 h for anti-cFos antibodies) at 4°C, and secondary antibodies were applied for 2 h at room temperature. The following primary antibodies were used: mouse anti-APC/CC1 Ab-7 (Millipore, OP80, 1:100), chicken anti-mCherry (Abcam, 205402, 1:1000), rat anti-Ctip2 monoclonal (Abcam, ab18465, 1:500), rabbit anti-cFos (synaptic system 226003, 1:1000) for P9 MS experiments, rabbit anti-cFos antiserum (Abcam, 190289, 1:1000) for DREADDs experiments, mouse anti-NeuN (US Biological, 1:600), rabbit anti-Olig2 (Millipore Ab9610, 1:1000), rat anti-PDGFRα (BD Bioscience, 558774, 1:600) and rabbit anti-Tbr1 (Abcam, 1:1000). The corresponding fluorescent donkey antisera secondary (Jackson ImmunoResearch, 1:200) were applied to visualize multiple markers in the same tissue without cross reactivity. Sections were subsequently mounted using the SlowFade (Molecular Probes 536939).

Images acquisition

Fluorescent images were acquired on a Leica SP5 confocal system equipped with an Argon laser (for the 488nm excitation), a Diode 561nm and HeNe 633nm. The Z-series stacks of confocal images were acquired at 1024 x 1024 pixels resolution, with a pinhole set to one Airy unit and optimal settings for gain and offset.

Acute slice preparation and electrophysiology

P9–P11 mice were sacrificed by decapitation and the brains were immediately removed from the skull and placed in oxygenated 4°C artificial cerebrospinal fluid (ACSF1), with the following concentrations in mM: 125 NaCl, 2.5 KCl, 25 glucose, 25 $NaHCO_3$, 1.25 NaH_2PO_4, 2 $CaCl_2$, and 1 $MgCl_2$, and continuously bubbled with 95% O_2-5% CO_2. Slices (250 µm) were cut using a vibroslicer (HM650V, Microm) and incubated at 32°C for 20 minutes and then at room temperature (20-25°C). For patch-clamp recordings, slices were transferred to the recording chamber and continuously superfused with ACSF2 (30-32°C), with the following concentrations in mM: 125 NaCl, 3.5 KCl, 25 glucose, 25 $NaHCO_3$, 1.25 NaH_2PO_4, 1 $CaCl_2$ and 0.5 $MgCl_2$, pH 7.2 and continuously bubbled with 95% O_2-5% CO_2. $mCherry^+$ neurons were visually identified using an upright microscope (BX 51, Olympus) equipped with standard epifluorescence. Thick-tufted layer 5 pyramidal neurons were identified based on their pyramid-like soma and stereotypical dendritic morphology with a prominent apical dendrite. Patch-clamp pipettes (4–6 Mohm resistance) were prepared from borosilicate glass (BF150-86-10; Harvard Apparatus) with a DMZ pipette puller (Zeitz). Patch-clamp experiments were performed using the following intracellular solution: 105 K-gluconate, 10 HEPES, 10 phosphocreatine-Na, 4 MgATP, 30 KCl (pH 7.25, adjusted with KOH). $GABA_A$ receptors were blocked with 10µm SR95531 hydrobromide (Gabazine, HelloBio), AMPA receptors with 10µM 6-cyano-7-nitroquinoxaline-2,3-dione (CNQX, HelloBio), and NMDA receptors with 50 µM d-APV (HelloBio). To activate DREADDs, $mCherry^+$ thick-tufted layer 5 pyramidal neurons were patch-clamped in the presence of CNO (30 µM) or clozapine (1 µM) in the ACSF2. The junction potential was not corrected for. Data acquisition was performed using Patchmaster software (Heka Elektronik). Signals were sampled at 20 kHz and filtered at 3 kHz, and off-line analysis was performed using Igor Pro (Wavemetrics).

Behavioral Studies

Female and male mice were tested separately for emotional behaviors following the series of behavioral tests starting at P80. Several cohorts were conducted for MS and SFR+hM4Di phenotype and none has undergone all the tests. For the single MS+hM3D cohort, the tests were performed in the following order: open-field, elevated plus maze, burying marble test, sequential objects recognition test, splash test and the two-days forced swim test, with 3 to 7 days between each test according to the stress of the test. All behavioral testing was done during the light cycle between 9 am and 6 pm and animals were transferred to the testing room in their home cage at least 30 min before the onset of the test for habituation. To eliminate odor cues, each apparatus was thoroughly cleaned with alcohol after each animal and males and females were conducted separately. Testing took place under ambient light conditions (50-80 lux).

Open Field test: Exploration and reactivity to a novel environment were assessed using an open field (OF) test. Mice were placed in the center of rectangular plastic grey boxes (H24,5xL35xL55cm) and activity was recorded for 20 min. Total distance and time spent in the center of the OF were automatically recorded using AnyMaze tracking software (Stoelting Co).

Elevated Plus Maze test: The maze is a grey plus-crossed-shaped apparatus, with two open arms (30 cm) and two closed arms (30 m) linked by a central platform and located 40cm above the floor. Mice were individually put in the center of the maze facing an open arm and were allowed to explore the maze for 10 min. The time spent and the entries into the open arms were automatically measured using AnyMaze tracking software and used as anxiety indexes.

Burying Marble test: Housing cages (20x36 cm) were filled with 6 cm of wood bedding (instead

of housing white chip cellulose bedding) and 3x4 marbles were evenly distributed as a grid. Mice were individually put in a corner of the cage and the number of marbles buried on more than 2/3 of their surface was manually recorded every minute for 20 min.

Splash Test: Group housed animals were placed in a new cage with bedding for at least 30 min in a room with dim light (40 lux). Mice were then individually sprayed on the back twice (~2x0,6 mL) with 20% sucrose solution in water and placed in a corner of their home cage. Grooming behaviors, including licking, stroking and scratching were manually recorded using AnyMaze software keys.

Sequential Novel Object Recognition test: This test is an adapted version of the novel object recognition test more specific to mPFC functioning and was performed as previously described [33]. Animals were first habituated to the arena (same grey boxes as OF), without stimuli for 10 min daily for 2 d before the commencement of the behavioral testing. This task comprised two sample phases and one test trial. In each sample phase, the subjects were allowed to explore two copies of an identical object for a total of 4 min. Different objects were used for sample phases 1 and 2 (miniature car then plastic hook, or glass tube then cork of Falcon tube), with a delay between the sample phases of 1h. The test trial (3 min) was given 3 h after sample phase 2. During the test trial, one copy of the objects from sample phase 1 and one copy of the objects from sample phase 2 were used. The positions of the two objects were counterbalanced between the animals. If temporal order memory is intact, the subjects will spend more time exploring the object from sample 1 (i.e., the object presented less recently) compared with the object from sample 2 (i.e., the novel object).

Porsolt Forced Swim test: Testing of behavioral despair was carried out in two consecutive days using a glass cylinder (40 cm X 20 cm diameter) filled with water (23-25°C) up to 3/4. Mice were tested once a day for 6 min. All the swim sessions were videotaped and manually tracked using AnyMaze software keys.

Statistics:

The Gaussian distributions of the values were tested on Prism software using d'Agostino and Pearson or Shapiro-Wilk for small n. T-test or ANOVA test were then performed when possible and otherwise Mann-Whitney test was applied and specified in the text. All results are expressed in mean ± sem. * $p<0.05$, ** $p<0.01$ and *** $p<0.005$.

Contributions

A.T. generated the cohorts and performed the histological and behavioral experiments and analyzed all the data. B.A.d.C. provided some useful help for the histological analysis. C.L.-M. and A.d.S. performed the electrophysiological recordings and analyzed the data. J.O. performed and analyzed the western blot experiments. Y.L. performed and analyzed the transcriptome profiling experiments. A.B. and V.V. helped designing the study. P.G. and A.T. designed the study and wrote the manuscript with the help of all authors.

Acknowledgements

We would like to thanks Dr. Macklin, Dr. Soiza-Reilly, Dr. Parras and Dr. Angulo for their scientific and technical advices. We are also thankful to the members of the CEF UMS28 facility as well as the U839 and U894 imaging plateforms for all their support. This work has been funded by the Labex BioPsy, the French Agence Nationale pour la Recherche (ANR) and the

Behavior and Brain Foundation Young Investigator-NARSAD Grant. B.A.d.C. received a scholarship from Coordination for the Improvement of Higher Education Personnel (CAPES), Brazil.

FIGURE LEGENDS

Figure 1: Analysis of differentially expressed genes in the mPFC of P15 animals exposed to maternal separation highlights myelin ensheathment and immediate early genes. A Scheme represents the experimental paradigm of the maternal separation (MS) versus standard facility raised (SFR) protocols as well as the dissection of mPFC at P15 to generate 4 samples per condition, each including 3 unilateral mPFC. B Graph shows with a log2 scale the fold change (FC) of expression induced by MS according to the number of reads detected in control samples for the genes with $q<0.05$ and $FC>1.3$ or $FC<0.7$. Myelin-ensheathment genes are highlighted in red and immediate early genes in blue. C and D Graphs show the qPCR results obtained in a second cohort to determine the expression levels of IEG (C) and genes related to myelin ensheathment (D).

Figure 2: Maternal separation induces precocious differentiation of oligodendrocytes in the developing mPFC. A Scheme represents the specificity of the oligodendrocyte lineage markers using triple immunostaining. Oligodendrocyte progenitor cells (OPC) express Olig2 and high levels of PDGFRα while mature oligodendrocytes (OL) express Olig2 and high levels of the CC1 antigen. Scale bar represents 20µm. B and C Graphs show the density of OPC (dark orange) and OL (light orange) in the P15 (B) and adult (C) mPFCs of SFR and MS animals. D Scheme represent the protocol of sequential labeling of OPC using IdU injections at P10 and BrdU injections at P15 to differentiate the fraction of P10 OPC that are still cycling at P15 (blue, IdU^+BrdU^+) from those which start differentiating by then (purple, IdU^+BrdU^-). E Graph shows an increased fraction of differentiated OPC in P15 mPFC of MS animals as compared to SFR animals.

Figure 3: Neuronal activity bi-directionally controls oligodendrocyte differentiation in the developing mPFC. A Scheme represents the experimental paradigms of the chronic treatment with CNO or SAL solutions from P12 to P14 after local and bilateral injections of pharmacogenetic virus. All animals were either exposed to inhibitory hM4D(Gi) virus and SFR protocol (blue, SFR+hM4Di) or exposed to excitatory hM3D(Gq) virus and MS protocol (red, MS+hM3Dq). B and C Images show mCherry labeling in P15 mPFC (B) and the specificity of viral expression to neuronal lineage by NeuN and mCherry co-labeling (C). Scale bars represent 500 µm (B) and 20 µm (C). D-G Graphs show the density of OPC (dark orange) and OL (light orange) in the P15 (D, F) and adult (E, G) mPFCs of SFR+hM4Di (D, E) and MS+hM3Dq (F, G) animals.

Figure 4: Early inhibition of mPFC neurons recapitulates the emotional disorders induced by early life stress. A Scheme represents the experimental paradigms of MS (orange) or

SFR+hM4Di (blue) animals exposed to behavioral tests in adulthood. B and B' Graphs show the distance travelled in an open field (OF) by SFR or MS animals (B) and by SFR+hM4Di animals exposed to chronic SAL or CNO (B'). C and C' Graphs show the time spent in the center of the OF during a 20min test. D and D' Graphs show the time spent in the open arm of an Elevated Plus Maze (EPM) during a 10min test. E and E' Graphs show the number of buried marbles at each minutes of a 15min test. F and F' Graphs show the time floating per min of a 6 min forced swim test (FST). G and G' Scheme represents the experimental paradigm of the sequential object recognition test with 3min of two identical Object1 exploration, followed 1h after by 3min of two identical Object 2 exploration, and 3h after by 4min of one Object1 and one Object2 exploration test. Graphs show the preference ratio for Object1.

Figure 5: Early activation of mPFC neurons prevents the emergence of the depression-like phenotype induced by early life stress. A Scheme represents the experimental paradigms of MS+hM3Dq animals exposed to behavioral tests in adulthood. B Graph show the distance travelled in an open field (OF) by MS+hM3Dq animals exposed to SAL (black) or CNO (red). C Graph shows the time spent in the center of the OF during a 20min test. D Graph shows the time spent in the open arm of an EPM during a 10min test. E Graph shows the number of buried marbles at each minutes of a 20min test. F Graph shows the time floating per min of a 6 min FST. G Graph shows the preference ratio for Object1. H and I Graphs show the cumulative time grooming after a splash with 20% sucrose solution by SFR+hM3Dq animals exposed to chronic SAL or CNO (H) and by SFR or MS animals (I).

REFERENCES

1 Norman RE, Byambaa M, De R, Butchart A, Scott J, Vos T. The long-term health consequences of child physical abuse, emotional abuse, and neglect: a systematic review and meta-analysis. *PLoS Med* 2012; **9**: e1001349.

2 Pechtel P, Pizzagalli DA. Effects of early life stress on cognitive and affective function: an integrated review of human literature. *Psychopharmacology (Berl)* 2011; **214**: 55–70.

3 Kessler RC, McLaughlin KA, Green JG, Gruber MJ, Sampson NA, Zaslavsky AM *et al.* Childhood adversities and adult psychopathology in the WHO World Mental Health Surveys. *Br J Psychiatry* 2010; **197**: 378–85.

4 Heim C, Shugart M, Craighead WE, Nemeroff CB. Neurobiological and psychiatric consequences of child abuse and neglect. *Dev Psychobiol* 2010; **52**: 671–90.

5 Insana SP, Banihashemi L, Herringa RJ, Kolko DJ, Germain A. Childhood maltreatment is associated with altered frontolimbic neurobiological activity during wakefulness in adulthood. *Dev Psychopathol* 2016; **28**: 551–64.

6 Nelson CA. Hazards to Early Development: The Biological Embedding of Early Life Adversity. *Neuron* 2017; **96**: 262–266.

7 Tanti A, Kim JJ, Wakid M, Davoli M-A, Turecki G, Mechawar N. Child abuse associates with an imbalance of oligodendrocyte-lineage cells in ventromedial prefrontal white matter. *Mol Psychiatry* 2017. doi:10.1038/mp.2017.231.

8 Syed SA, Nemeroff CB. Early Life Stress, Mood, and Anxiety Disorders. *Chronic Stress*

2017; **1**: 247054701769446.

9 Gutman DA, Nemeroff CB. Neurobiology of early life stress: rodent studies. *Semin Clin Neuropsychiatry* 2002; **7**: 89–95.

10 Callaghan BL, Sullivan RM, Howell B, Tottenham N. The international society for developmental psychobiology Sackler symposium: early adversity and the maturation of emotion circuits--a cross-species analysis. *Dev Psychobiol* 2014; **56**: 1635–50.

11 Tractenberg SG, Levandowski ML, de Azeredo LA, Orso R, Roithmann LG, Hoffmann ES *et al.* An overview of maternal separation effects on behavioural outcomes in mice: Evidence from a four-stage methodological systematic review. *Neurosci Biobehav Rev* 2016; **68**: 489–503.

12 Bordner K a., George ED, Carlyle BC, Duque A, Kitchen RR, Lam TT *et al.* Functional genomic and proteomic analysis reveals disruption of myelin-related genes and translation in a mouse model of early life neglect. *Front Psychiatry* 2011; **2**: 1–18.

13 Braun K, Bock J. The experience-dependent maturation of prefronto-limbic circuits and the origin of developmental psychopathology: implications for the pathogenesis and therapy of behavioural disorders. *Dev Med Child Neurol* 2011; **53**: 14–18.

14 Sood A, Pati S, Bhattacharya A, Chaudhari K, Vaidya VA. Early emergence of altered 5-HT2A receptor-evoked behavior, neural activation and gene expression following maternal separation. *Int J Dev Neurosci* 2018; **65**: 21–28.

15 Molet J, Maras PM, Avishai-Eliner S, Baram TZ. Naturalistic rodent models of chronic early-life stress. *Dev Psychobiol* 2014; **56**: 1675–88.

16 Carr CP, Martins CMS, Stingel AM, Lemgruber VB, Juruena MF. The role of early life stress in adult psychiatric disorders: a systematic review according to childhood trauma subtypes. *J Nerv Ment Dis* 2013; **201**: 1007–20.

17 Chocyk A, Majcher-Maoelanka I, Dudys D, Przyborowska A, Wêdzony K. Impact of early-life stress on the medial prefrontal cortex functions-a search for the pathomechanisms of anxiety and mood disorders. *Pharmacol Reports* 2013; **65**: 1462–1470.

18 Reincke SAJ, Hanganu-Opatz IL. Early-life stress impairs recognition memory and perturbs the functional maturation of prefrontal-hippocampal-perirhinal networks. *Sci Rep* 2017; **7**: 42042.

19 Holland FH, Ganguly P, Potter DN, Chartoff EH, Brenhouse HC. Early life stress disrupts social behavior and prefrontal cortex parvalbumin interneurons at an earlier time-point in females than in males. *Neurosci Lett* 2014; **566**: 131–6.

20 Yang Y, Cheng Z, Tang H, Jiao H, Sun X, Cui Q *et al.* Neonatal Maternal Separation Impairs Prefrontal Cortical Myelination and Cognitive Functions in Rats Through Activation of Wnt Signaling. *Cereb Cortex* 2017; **27**: 2871–2884.

21 Takesian AE, Hensch TK. *Changing Brains - Applying Brain Plasticity to Advance and Recover Human Ability*. Elsevier, 2013 doi:10.1016/B978-0-444-63327-9.00001-1.

22 Gaspar P, Cases O, Maroteaux L. The developmental role of serotonin: news from mouse molecular genetics. *Nat Rev Neurosci* 2003; **4**: 1002–1012.

23 Sarro EC, Wilson DA, Sullivan RM. Maternal Regulation of Infant Brain State. *Curr Biol* 2014; **24**: 1664–1669.

24 Horii-Hayashi N, Sasagawa T, Matsunaga W, Matsusue Y, Azuma C, Nishi M. Developmental Changes in Desensitisation of c-Fos Expression Induced by Repeated Maternal Separation in Pre-Weaned Mice. *J Neuroendocrinol* 2013; **25**: 158–167.

25 Armbruster BN, Li X, Pausch MH, Herlitze S, Roth BL. Evolving the lock to fit the key to

create a family of G protein-coupled receptors potently activated by an inert ligand. *Proc Natl Acad Sci U S A* 2007; **104**: 5163–5168.

26 Risso D, Ngai J, Speed TP, Dudoit S. Normalization of RNA-seq data using factor analysis of control genes or samples. *Nat Biotechnol* 2014; **32**: 896–902.

27 Hill RA, Patel KD, Goncalves CM, Grutzendler J, Nishiyama A. Modulation of oligodendrocyte generation during a critical temporal window after NG2 cell division. *Nat Neurosci* 2014; **17**: 1518–1527.

28 Silbereis JC, Huang EJ, Back SA, Rowitch DH. Towards improved animal models of neonatal white matter injury associated with cerebral palsy. *Dis Model Mech* 2010; **3**: 678–88.

29 Mount CW, Monje M. Wrapped to Adapt: Experience-Dependent Myelination. *Neuron* 2017; **95**: 743–756.

30 Roth BL. DREADDs for Neuroscientists. *Neuron* 2016; **89**: 683–694.

31 Stachniak TJ, Ghosh A, Sternson SM. Chemogenetic Synaptic Silencing of Neural Circuits Localizes a Hypothalamus→Midbrain Pathway for Feeding Behavior. *Neuron* 2014; **82**: 797–808.

32 Fernández-Alacid L, Watanabe M, Molnár E, Wickman K, Luján R. Developmental regulation of G protein-gated inwardly-rectifying K+ (GIRK/Kir3) channel subunits in the brain. *Eur J Neurosci* 2011; **34**: 1724–36.

33 Barker GRI, Bird F, Alexander V, Warburton EC. Recognition Memory for Objects, Place, and Temporal Order: A Disconnection Analysis of the Role of the Medial Prefrontal Cortex and Perirhinal Cortex. *J Neurosci* 2007; **27**: 2948–2957.

34 David DJ, Samuels BA, Rainer Q, Wang J, Marsteller D, Mendez I *et al.* Neurogenesis-Dependent and Independent. 2010; **62**: 479–493.

35 Suri D, Teixeira CM, Cagliostro MKC, Mahadevia D, Ansorge MS. Monoamine-Sensitive Developmental Periods Impacting Adult Emotional and Cognitive Behaviors. *Neuropsychopharmacology* 2014; **40**: 88–112.

36 Roque S, Mesquita AR, Palha JA, Sousa N, Correia-Neves M. The Behavioral and Immunological Impact of Maternal Separation: A Matter of Timing. *Front Behav Neurosci* 2014; **8**. doi:10.3389/fnbeh.2014.00192.

37 Makinodan M, Rosen KM, Ito S, Corfas G. A Critical Period for Social Experience-Dependent Oligodendrocyte Maturation and Myelination. *Science (80-)* 2012; **337**: 1357–1360.

38 Lehmann ML, Weigel TK, Elkahloun AG, Herkenham M. Chronic social defeat reduces myelination in the mouse medial prefrontal cortex. *Sci Rep* 2017; **7**: 46548.

39 Liu J, Dupree JL, Gacias M, Frawley R, Sikder T, Naik P *et al.* Clemastine Enhances Myelination in the Prefrontal Cortex and Rescues Behavioral Changes in Socially Isolated Mice. *J Neurosci* 2016; **36**: 957–962.

40 Barrera K, Chu P, Abramowitz J, Steger R, Ramos RL, Brumberg JC. Organization of myelin in the mouse somatosensory barrel cortex and the effects of sensory deprivation. *Dev Neurobiol* 2013; **73**: 297–314.

41 Kikusui T, Kiyokawa Y, Mori Y. Deprivation of mother–pup interaction by early weaning alters myelin formation in male, but not female, ICR mice. *Brain Res* 2007; **1133**: 115–122.

42 Miki T, Yokoyama T, Kusaka T, Suzuki S, Ohta K, Warita K *et al.* Early postnatal repeated maternal deprivation causes a transient increase in OMpg and BDNF in rat cerebellum suggesting precocious myelination. *J Neurol Sci* 2014; **336**: 62–67.

43 Bath KG, Manzano-Nieves G, Goodwill H. Early life stress accelerates behavioral and neural maturation of the hippocampus in male mice. *Horm Behav* 2016; **82**: 64–71.
44 Kikusui T, Mori Y. Behavioural and neurochemical consequences of early weaning in rodents. *J Neuroendocrinol* 2009; **21**: 427–31.
45 Minatohara K, Akiyoshi M, Okuno H. Role of Immediate-Early Genes in Synaptic Plasticity and Neuronal Ensembles Underlying the Memory Trace. *Front Mol Neurosci* 2016; **8**. doi:10.3389/fnmol.2015.00078.
46 Gibson EM, Purger D, Mount CW, Goldstein AK, Lin GL, Wood LS *et al.* Neuronal Activity Promotes Oligodendrogenesis and Adaptive Myelination in the Mammalian Brain. *Science (80-)* 2014; **344**: 1252304–1252304.
47 Xiao L, Ohayon D, McKenzie IA, Sinclair-Wilson A, Wright JL, Fudge AD *et al.* Rapid production of new oligodendrocytes is required in the earliest stages of motor-skill learning. *Nat Neurosci* 2016; **19**: 1210–1217.
48 He M, McCarthy KD. Oligodendroglial signal transduction systems are developmentally regulated. *J Neurochem* 1994; **63**: 501–8.
49 Wright J, Zhang G, Yu T-S, Kernie SG. Age-Related Changes in the Oligodendrocyte Progenitor Pool Influence Brain Remodeling after Injury. *Dev Neurosci* 2010; **32**: 499–509.
50 Orduz D, Maldonado PP, Balia M, Vélez-Fort M, de Sars V, Yanagawa Y *et al.* Interneurons and oligodendrocyte progenitors form a structured synaptic network in the developing neocortex. *Elife* 2015; **4**. doi:10.7554/eLife.06953.
51 Kuhlman SJ, Olivas ND, Tring E, Ikrar T, Xu X, Trachtenberg JT. A disinhibitory microcircuit initiates critical-period plasticity in the visual cortex. *Nature* 2013; **501**: 543–546.
52 Thompson AD, Picard N, Min L, Fagiolini M, Chen C. Cortical Feedback Regulates Feedforward Retinogeniculate Refinement. *Neuron* 2016; **91**: 1021–1033.
53 Fields RD. White matter in learning, cognition and psychiatric disorders. *Trends Neurosci* 2008; **31**: 361–370.
54 Schubert D, Martens GJM, Kolk SM. Molecular underpinnings of prefrontal cortex development in rodents provide insights into the etiology of neurodevelopmental disorders. *Mol Psychiatry* 2015; **20**: 795–809.
55 Puig MV, Gulledge AT. Serotonin and Prefrontal Cortex Function: Neurons, Networks, and Circuits. *Mol Neurobiol* 2011; : 1–16.
56 Edgar NM, Touma C, Palme R, Sibille E. Resilient emotionality and molecular compensation in mice lacking the oligodendrocyte-specific gene Cnp1. *Transl Psychiatry* 2011; **1**: e42–e42.
57 Chen X, Zhang W, Li T, Guo Y, Tian Y, Wang F *et al.* Impairment of Oligodendroglia Maturation Leads to Aberrantly Increased Cortical Glutamate and Anxiety-Like Behaviors in Juvenile Mice. *Front Cell Neurosci* 2015; **9**. doi:10.3389/fncel.2015.00467.
58 Dries DR, Zhu Y, Brooks MM, Forero DA, Adachi M, Cenik B *et al.* Loss of Nicastrin from Oligodendrocytes Results in Hypomyelination and Schizophrenia with Compulsive Behavior. *J Biol Chem* 2016; **291**: 11647–56.
59 Gould EA, Busquet N, Shepherd D, Dietz RM, Herson PS, Simoes de Souza FM *et al.* Mild myelin disruption elicits early alteration in behavior and proliferation in the subventricular zone. *Elife* 2018; **7**. doi:10.7554/eLife.34783.
60 Birey F, Kloc M, Chavali M, Hussein I, Wilson M, Christoffel DJ *et al.* Genetic and Stress-Induced Loss of NG2 Glia Triggers Emergence of Depressive-like Behaviors

through Reduced Secretion of FGF2. *Neuron* 2015; **88**: 941–956.

61 Laine MA, Trontti K, Misiewicz Z, Sokolowska E, Kulesskaya N, Heikkinen A *et al.* Genetic Control of Myelin Plasticity after Chronic Psychosocial Stress. *eneuro* 2018; **5**: ENEURO.0166-18.2018.

62 Anders S, Pyl PT, Huber W. HTSeq--a Python framework to work with high-throughput sequencing data. *Bioinformatics* 2015; **31**: 166–9.

63 Robinson MD, McCarthy DJ, Smyth GK. edgeR: a Bioconductor package for differential expression analysis of digital gene expression data. *Bioinformatics* 2010; **26**: 139–140.

64 Storey JD, Tibshirani R. Statistical significance for genomewide studies. *Proc Natl Acad Sci* 2003; **100**: 9440–9445.

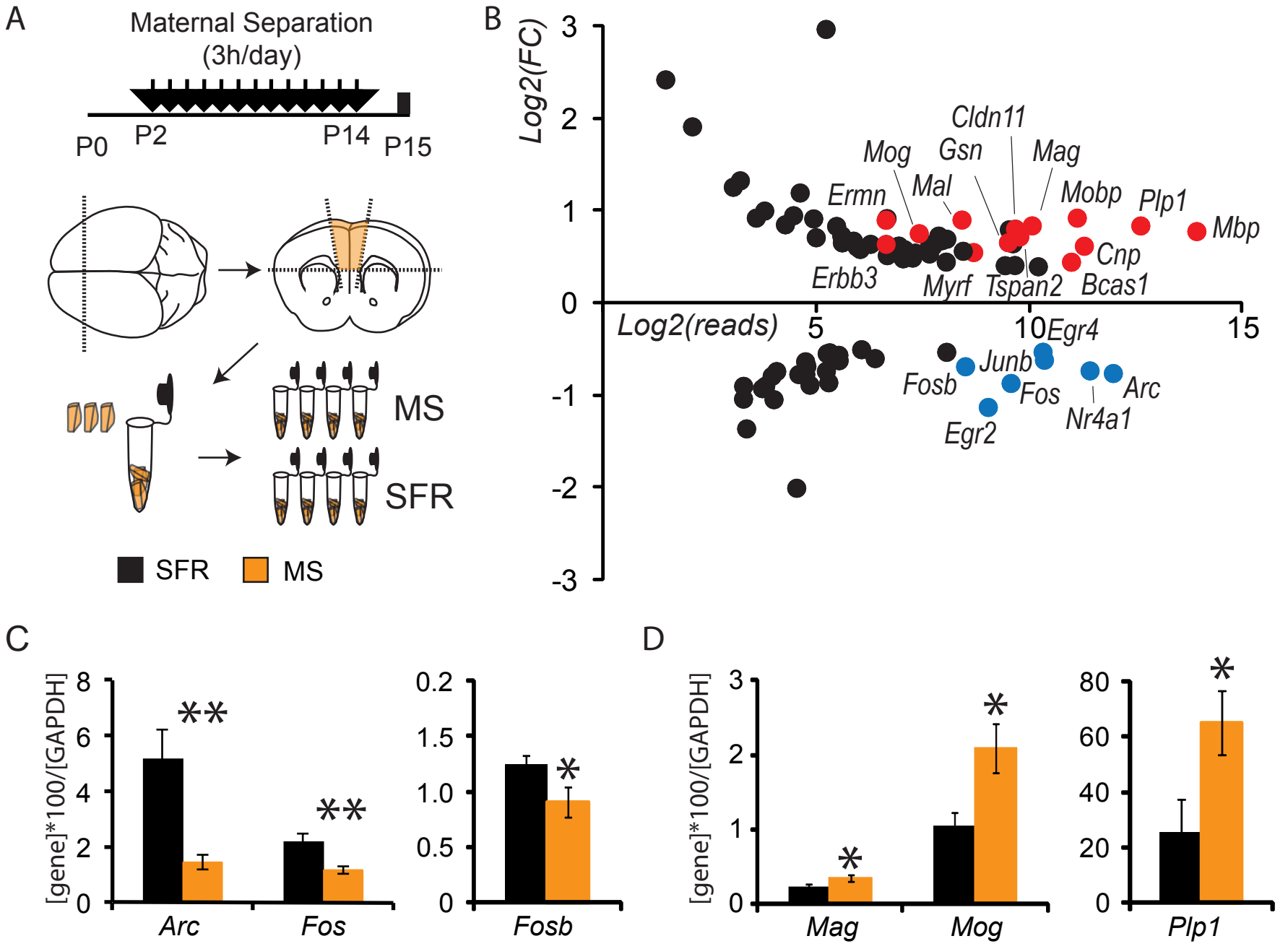

Figure 1: Analysis of differentially expressed genes in the mPFC of P15 animals exposed to maternal separation highlights myelin ensheathment and immediate early genes.

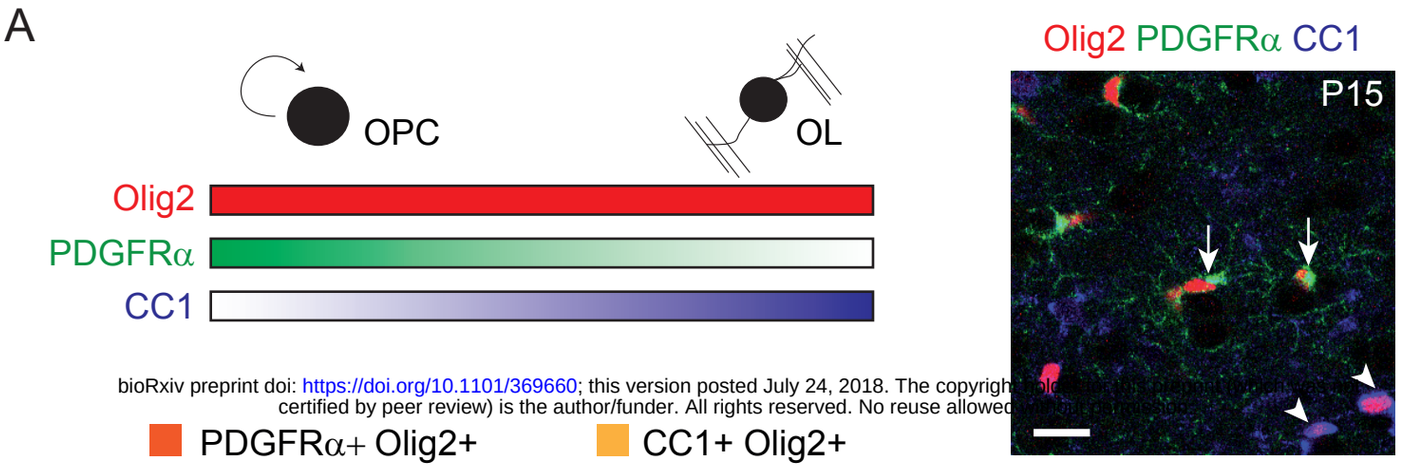

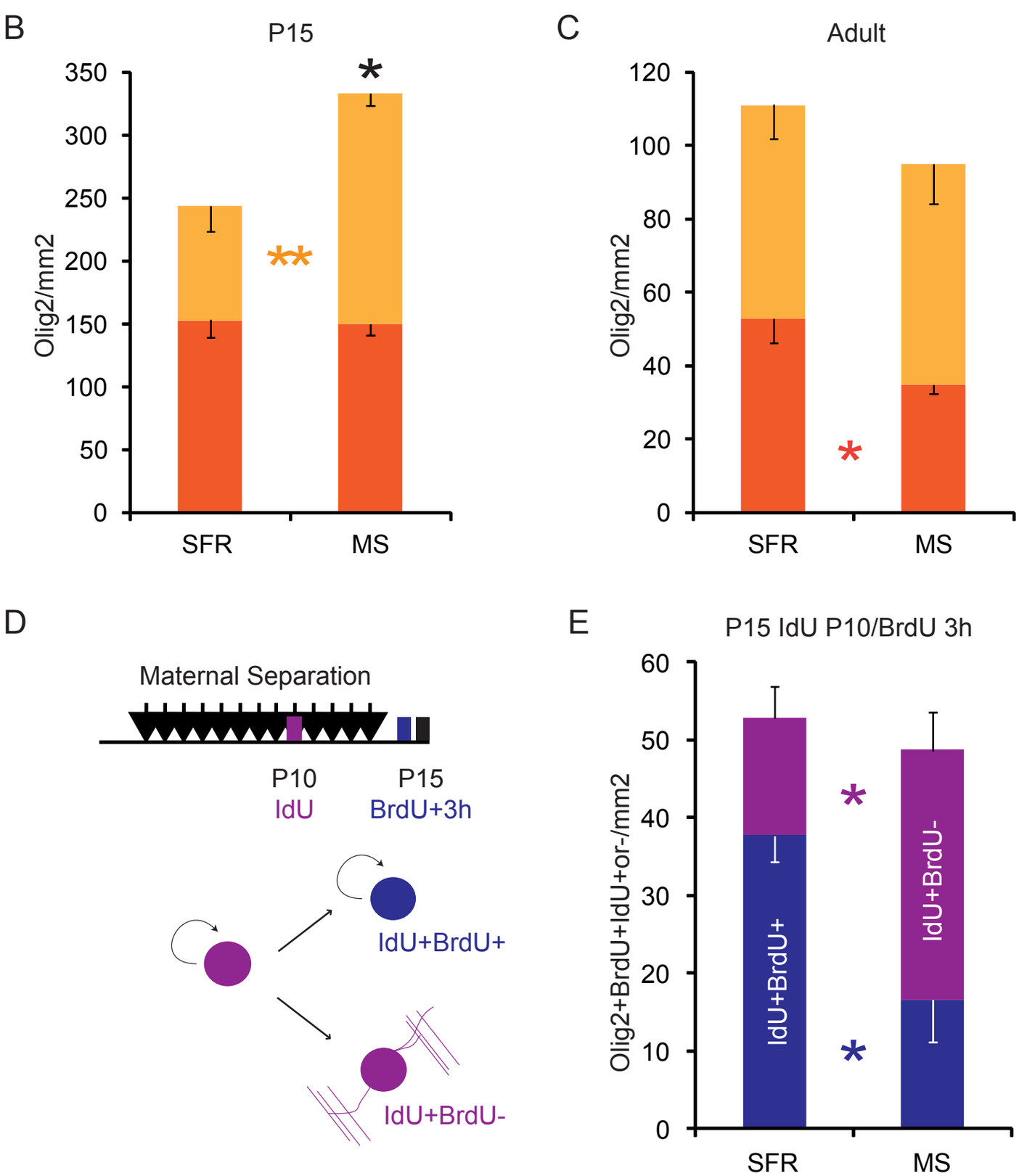

Figure 2: Maternal separation induces precocious differentiation of oligodendrocytes in the developing mPFC.

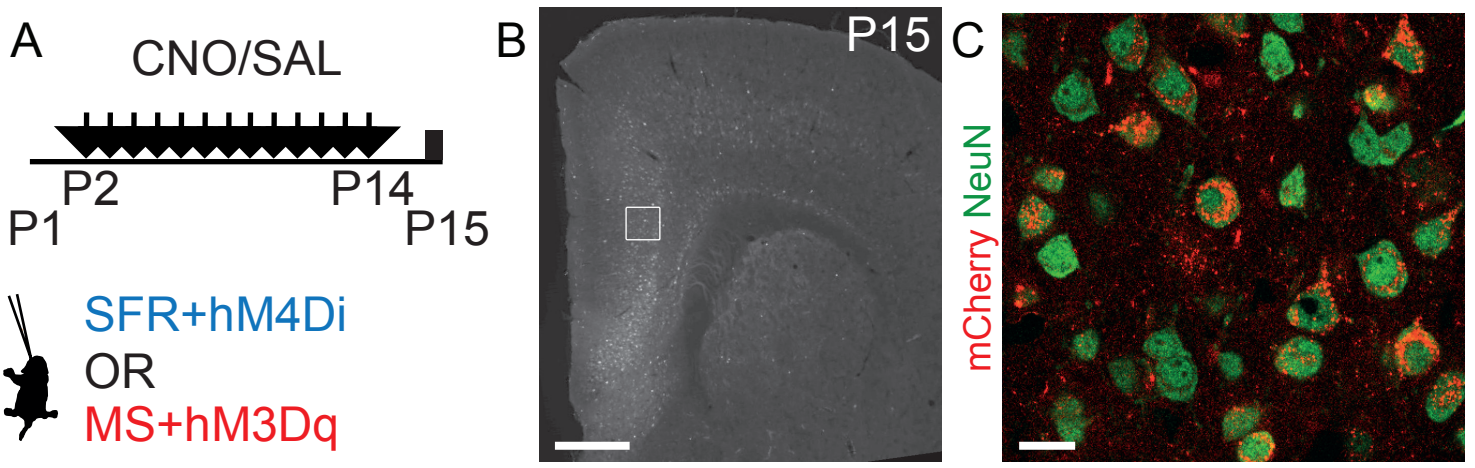

P15 Adult

SFR+hM4Di

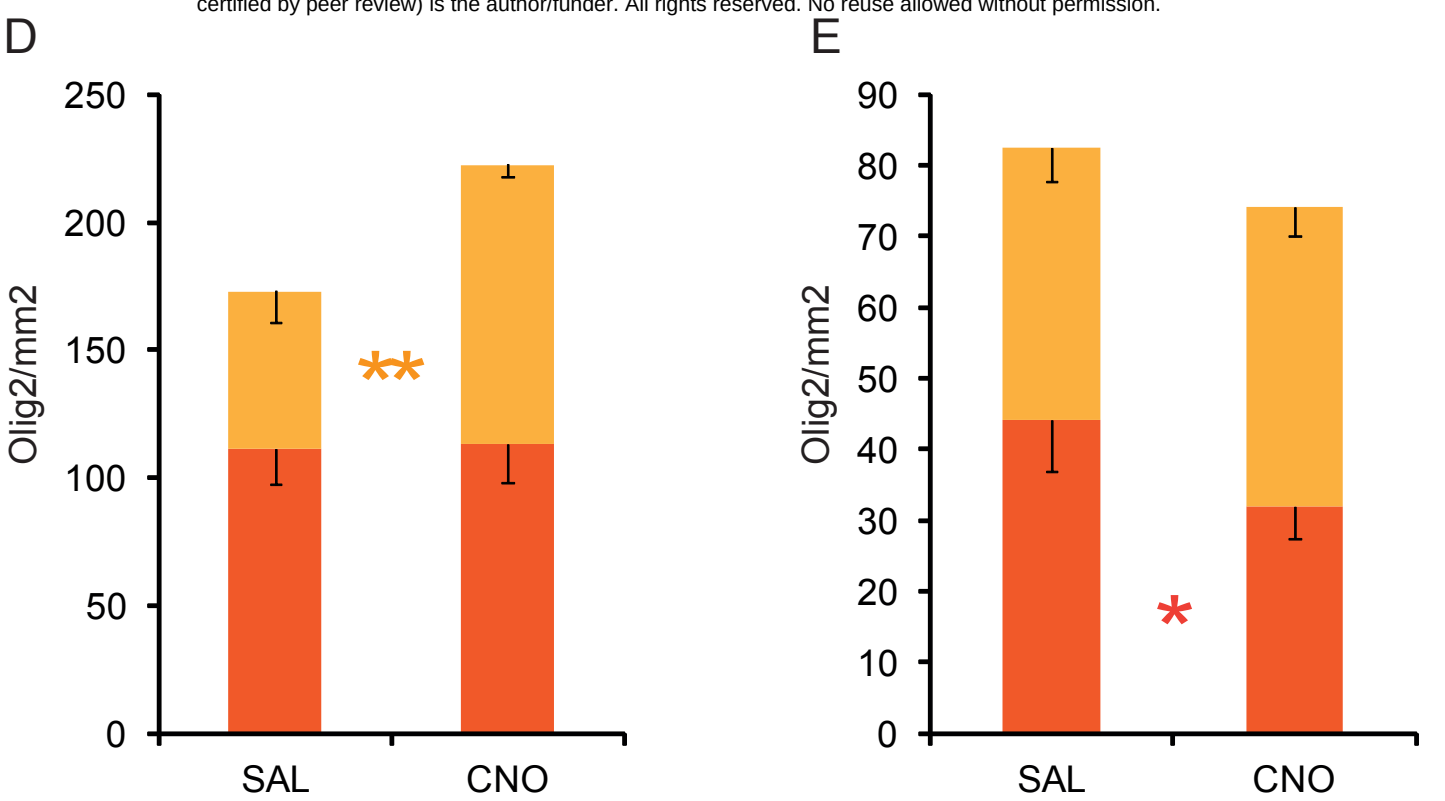

MS+hM3Dq

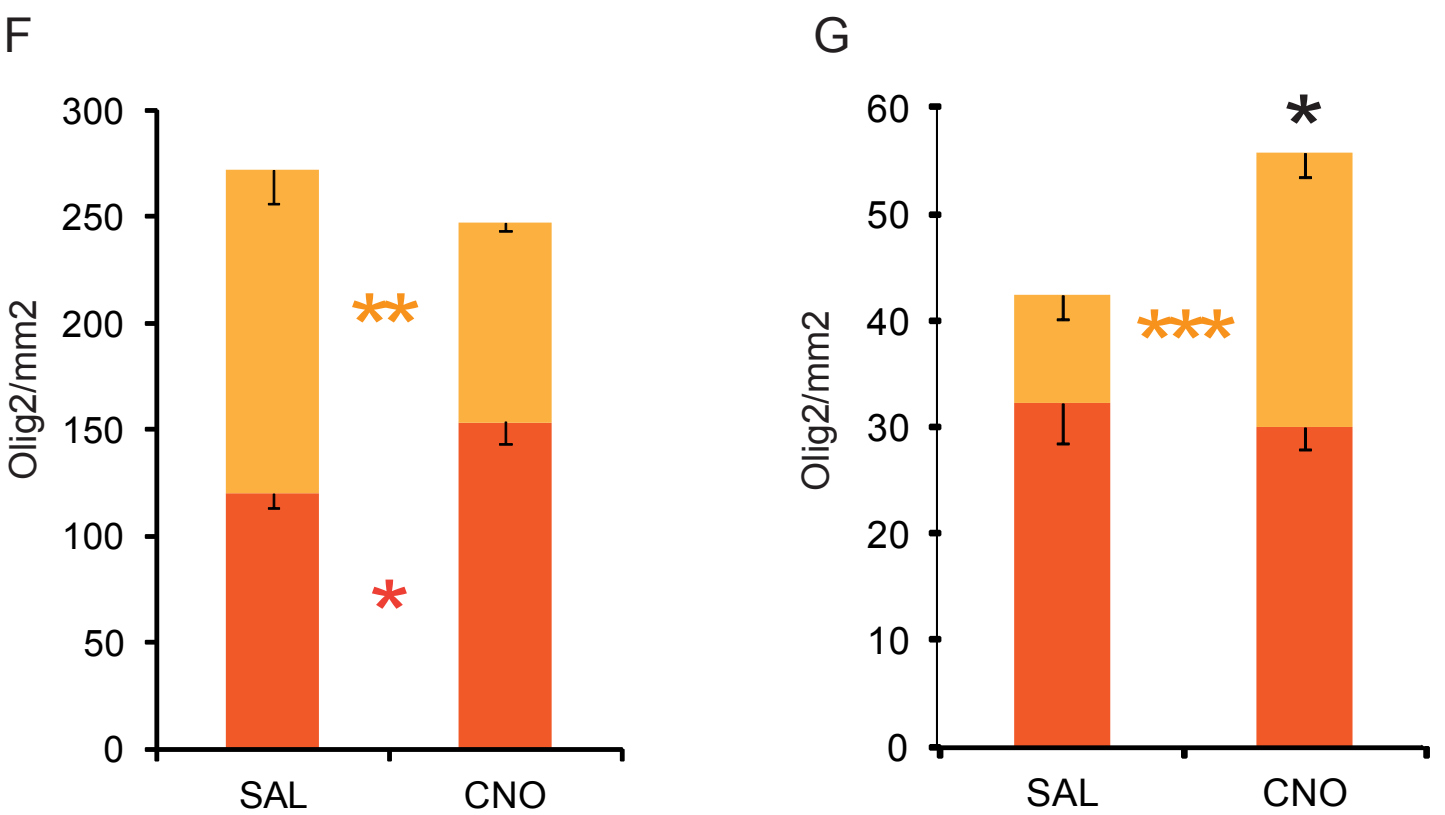

Figure 3: Neuronal activity bi-directionally controls oligodendrocyte differentiation in the developing mPFC.

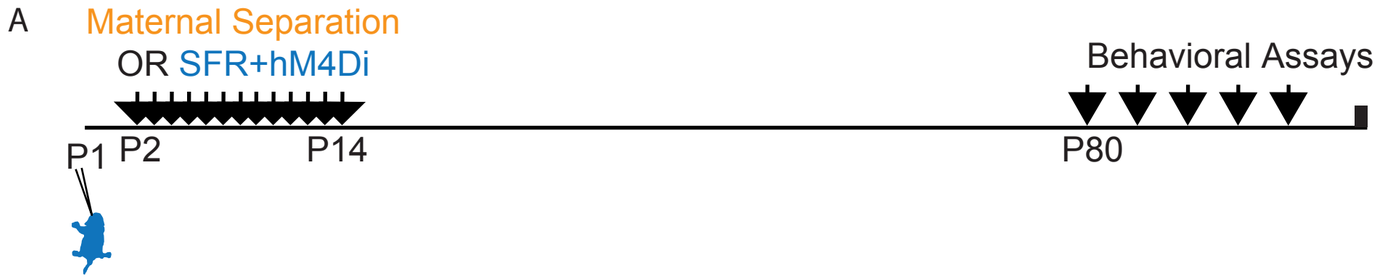

OF Distance (m/20min) | OF Center time (sec/20min) | EPM Open arm time (sec/10min) | # Marbles burried (per min)

Maternal Separation

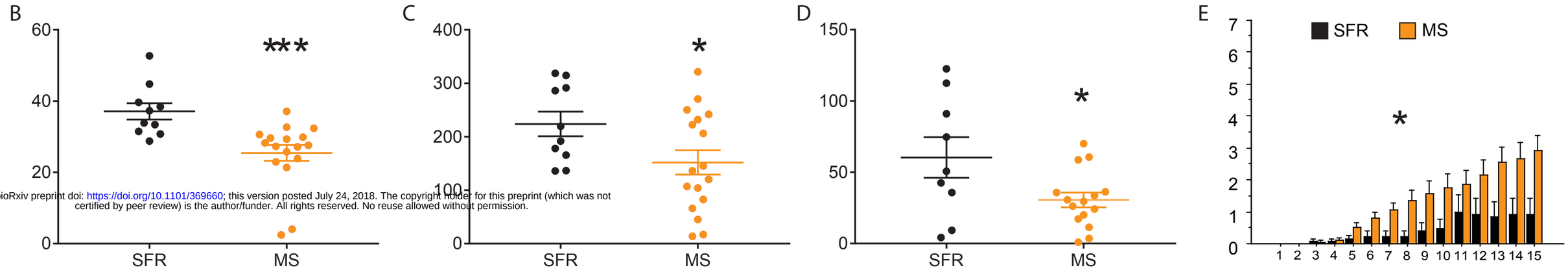

SFR+hM4Di

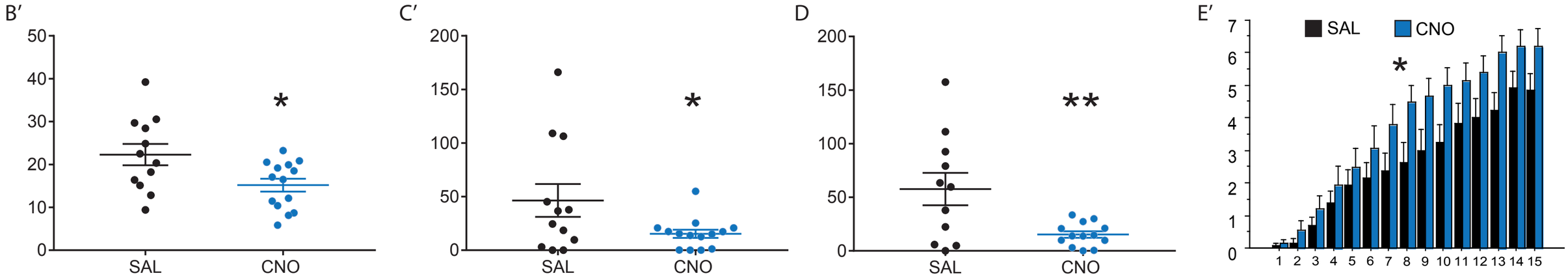

FST Floating time (sec/min)

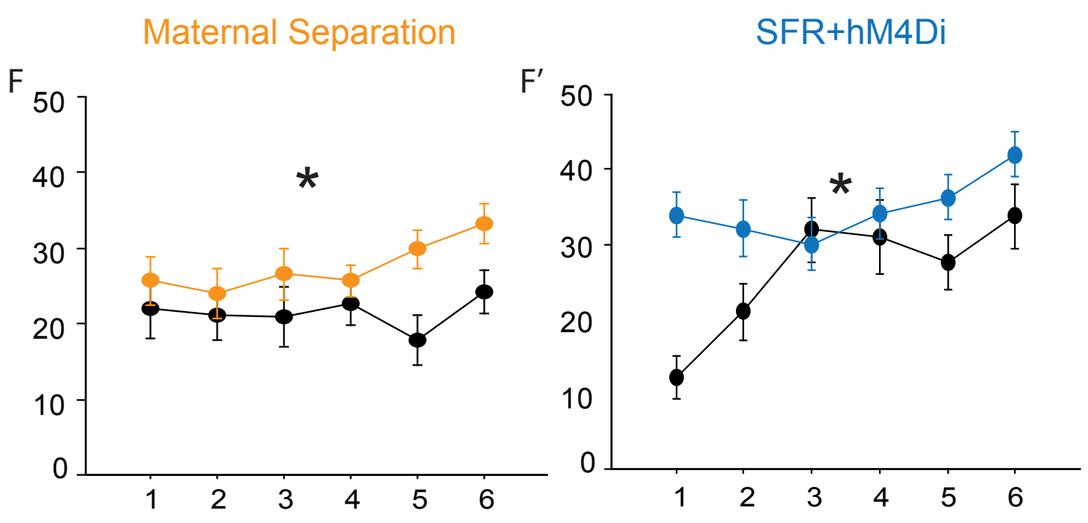

Sequential object preference
(T1-T2)*100/(T1+T2)

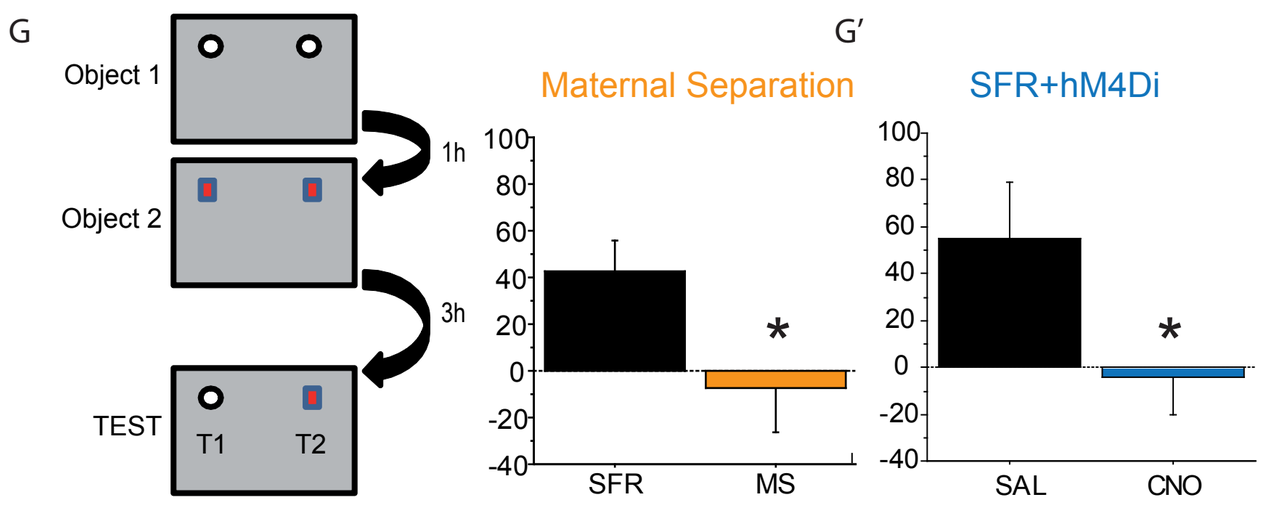

Figure 4: Early inhibition of mPFC neurons recapitulates the emotional disorders induced by early life stress.

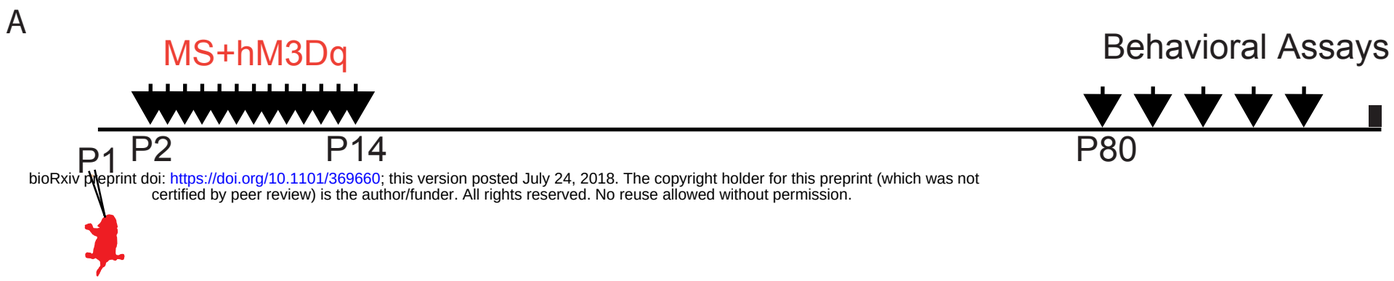

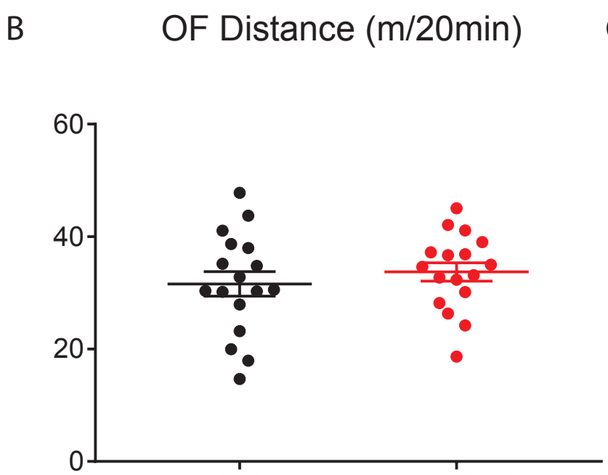

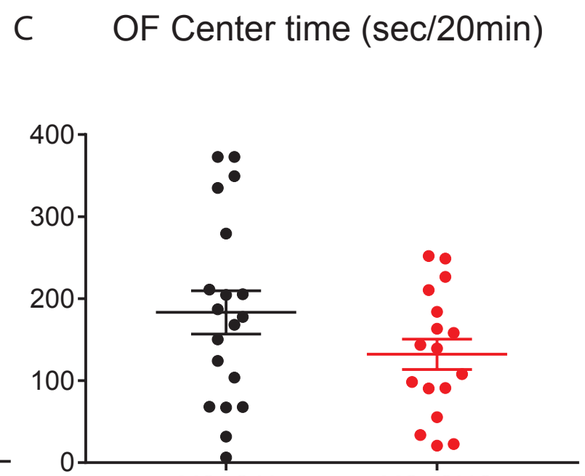

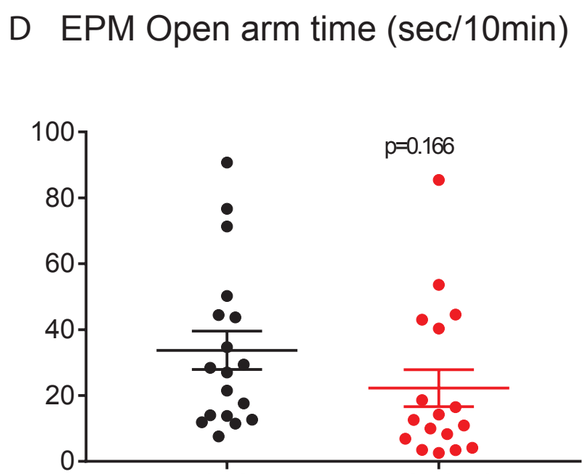

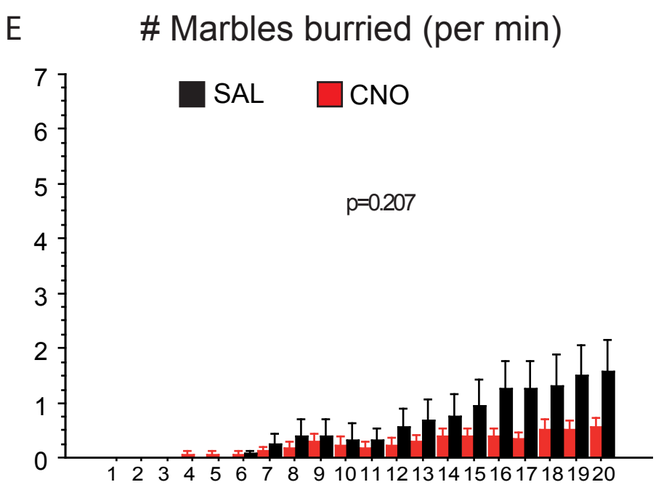

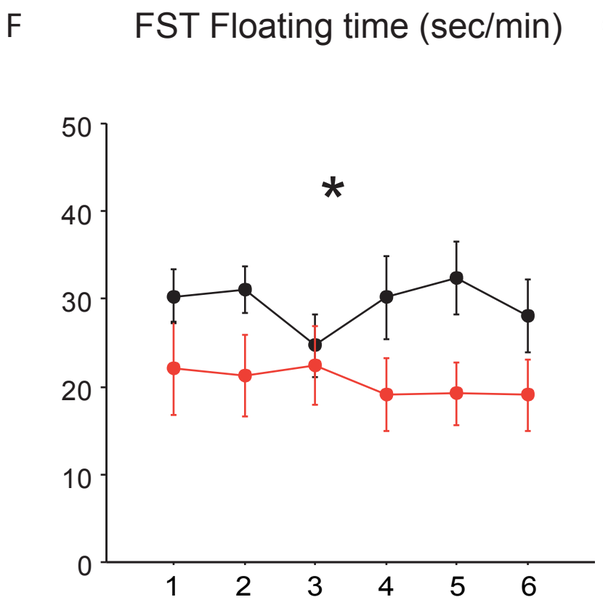

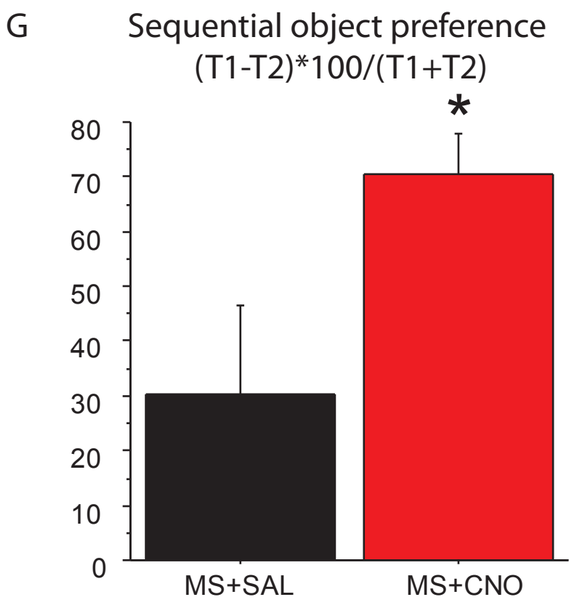

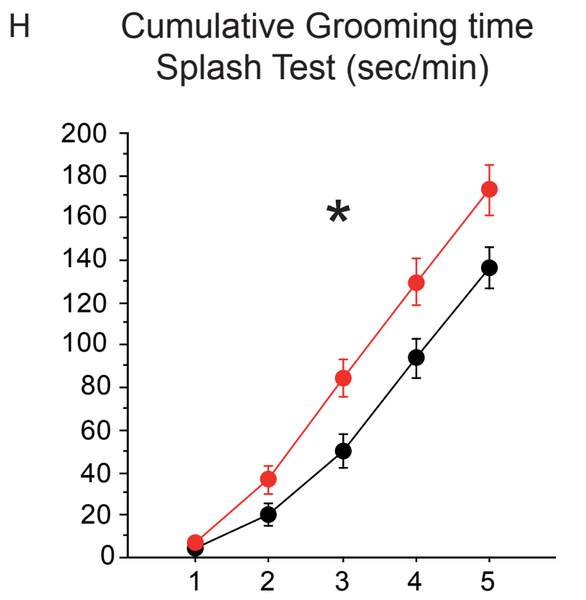

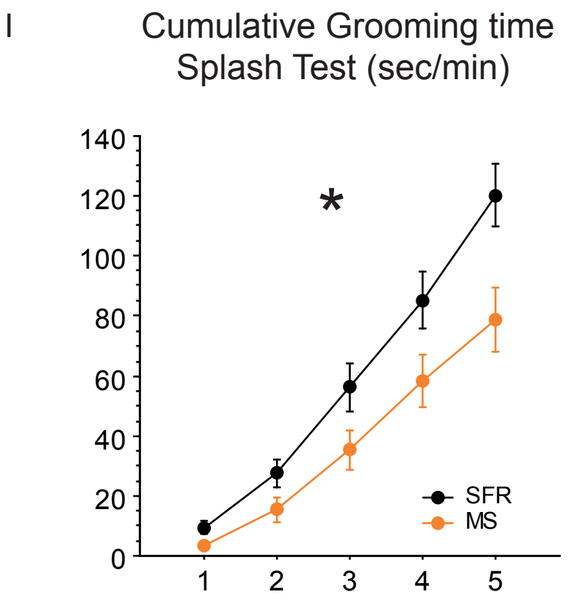

Figure 5: Early activation of mPFC neurons prevents the emergence of the depression-like phenotype induced by early life stress.